A New Approach to Modeling LGMDR1: Pyrvinium-Treated *capn3b* crispant Zebrafish

Ruiz-Roldán Cristina[1], Valls Andrea[1,2], Immanuel Jenita[1,2], De Santis Flavia[3], Fernández-Torrón Roberto[1,2,4], López de Munain Adolfo[1,2,4,5,6], Saenz Amets[1,2].

[1]Neuromuscular Diseases Group, Neurosciences Area, Biogipuzkoa Health Research Institute, San Sebastian, Spain
[2]CIBERNED, CIBER, Spanish Ministry of Science & Innovation, Carlos III Health Institute, Madrid, Spain
[3]ZeClinics S.L., Sant Feliu de Llobregat, Spain
[4]Department of Neurology, Donostialdea Integrated Health Organisation, Osakidetza, San Sebastian, Spain
[5]Department of Neurosciences, University of the Basque Country UPVEHU, San Sebastian, Spain
[6]Faculty of Medicine, University of Deusto, Bilbao, Spain

Corresponding author:

Amets Sáenz, Neurosciences Area, Biogipuzkoa Health Research Institute,

P° Dr Begiristain s/n, 20014 San Sebastian, Spain.

Email: amets.saenzpena@osakidetza.eus

Abstract

The lack of an accurate animal model for LGMDR1 is a major obstacle to therapeutic development. While murine models do not replicate the human gene expression profile, zebrafish offers a promising alternative. We generated a *capn3b* mutant zebrafish, which showed minimal phenotypic changes. However, when this model was treated with pyrvinium, a Wnt signaling inhibitor, its gene expression patterns mimic those observed in LGMDR1 patients, reinforcing the role of the Wnt pathway in LGMDR1 pathology. This pharmacologically enhanced model, despite lacking a clear phenotype in young larvae, could serve as a valuable tool for identifying potential therapeutic targets upon further investigation and validation.

INTRODUCTION

Limb-girdle muscular dystrophy R1 calpain 3-related (LGMDR1) is an autosomal recessive muscular dystrophy due to mutations in *CAPN3* that causes progressive degeneration of the proximal muscles. For most patients, onset occurs in the second decade of life and as muscle degeneration progresses; patients require a wheelchair for mobility after around 20 years of disease progression [1, 2].

CAPN3 is a muscle-specific protease [3] whose function in muscle is not completely understood. However, it has been reported that a lack of CAPN3 alters several structures, gene expression and signaling pathways in the skeletal muscle [4–7].

To advance the development of effective treatments for any disease, a biologically relevant *in vivo* model is essential. However, finding an animal model that perfectly mimics the clinical features of calpainopathies remains elusive.

Previous attempts have used various murine models to approximate the human condition and study the effects of *CAPN3* gene alterations. However, none have fully replicated the human phenotype [4, 8–11]. Even though DNA microarray analyses were performed to establish expression profiles in mouse models, unfortunately, these failed to reflect the gene expression patterns seen in human muscle [5, 10, 12].

This difficulty is also noticeable in zebrafish, which have two *CAPN3* homologs, *capn3a* and *capn3b*, although only *capn3b* is expressed in muscle. Earlier studies on a *capn3b*-deficient zebrafish model focused on its role in other processes, such as the calpain3 involvement in the nucleolar degradation pathway of p53, liver regeneration, and autoimmune responses [13–15]. More recently, RNA-less and partial deletion *capn3b* mutants were generated using CRISPR/Cas9 mutagenesis. While this model showed no significant muscular dystrophy phenotypes under normal conditions, it was more susceptible to muscle damage under challenging conditions, such as in mechanical stress situations [16].

It is known that a correct muscle fibre function requires a delicate balance between muscle protein synthesis and proteolysis by means of the Akt/mTOR and the Wnt/β-catenin signaling pathway, among others [17–19]. Both signaling pathways are altered in LGMDR1 patient's muscles. This could be due to the overexpression of FRZB, a Wnt

signalling pathway inhibitor, and to the reduction of mTOR and downstream kinases phosphorylation in LGMDR1 patients [5, 6, 20].

We generated a new *capn3b* crispant that, as the previous model, did not accurately reflect the phenotypic characteristics of the disease. To solve this problem, we have developed a pharmacologically enhanced zebrafish model, specifically designed to mimic an impaired signaling described in patients. Therefore, we focused on the Wnt signaling pathway inhibition by means of pyrvinium. When this zebrafish model was treated with pyrvinium, the gene expression deregulation demonstrated a greater resemblance to the deregulated patterns observed in LGMDR1 patients' muscles. This finding suggests that modulation of the Wnt signaling pathway may represent a promising therapeutic target for LGMDR1.

MATERIALS AND METHODS

Zebrafish Husbandry and Breeding

Adult wild-type AB strain zebrafish were maintained at 28.5 ± 1ºC in a 14 h light/10 h dark cycle in a closed recirculating tank system, according to standard protocols [21].

Generation of Crispants

Wild-type or Casper one-cell-stage embryos were injected following published protocols [22, 23] with a mix containing the Cas9 and sgRNAs targeting the coding sequence of the gene of interest or the Cas9 and a control sgRNA (scramble) (Table S1).

Mutation rates quantification

Genomic DNA was extracted from ten individual embryos at the stage of 24 hpf. The target region was amplified by PCR employing the primers capn3b-fw and capn3b-rev. The percentage of mutated alleles present in the PCR was quantified using the Synthego ICE analysis tool upon sequencing of the resulting amplicons.

Treatment

Pyrvinium pamoate salt hydrate was reconstituted in Dimethyl Sulfoxide (DMSO) to a stock concentration of 1mM and diluted in E3 1X medium to a final concentration of 0.400, 0.200, 0.100, 0.050, and 0.025 μM. 0.1% DMSO in E3 1X medium. 48 hpf larvae injected with scrambled sgRNA and capn3b sgRNAs were treated with 0.1% DMSO and with each of the Pyrvinium concentrations, they were maintained at 28.5ºC with a 14:10 hour light:dark cycle. The medium was renewed at 72, 96, and 120 hpf.

Morphological Analysis: birefringence

Larvae were anesthetized with tricaine 0.28 mg/mL, and images were captured using a stereomicroscope. After the imaging, larvae were euthanized and the birefringence was quantified as follows in Berger et al 2012 [24].

Analysis of locomotor activity

For the locomotion analysis, the standardized 25 min dark/light cycles paradigm (5 min darkness—5 min light up to 25 min) was used, the employed methodology was based on the protocol described in Locubiche *et al.,* 2024 [23].

Statistical analysis

Statistical analysis, from locomotor activity, were performed using One way ANOVA followed by Sidak's test.

For the study of the gene expression levels, data were expressed as the mean ± standard error of the mean (SEM) of three technical replicates. Statistical significance was determined using unpaired T-test, and a p-value < 0.05 was considered statistically significant. All computational analyses were performed using GraphPad Prism.

RNA extraction

For RNA extraction, 16 zebrafish larvae were used per condition. The PicoPureTM RNA Isolation Kit (Applied Biosystems, Thermo Fisher Scientific, Foster City, CA, EE. UU.) was used, following the manufacturer's instructions for RNA extraction.

RT-qPCR

The High-Capacity cDNA Reverse Transcription Kit (Life Technologies, Carlsbad, CA, EE. UU.) was used for cDNA synthesis, following the manufacturer's instructions.

To study gene expression levels by qRT-PCR, *SYBR Green* primers (Table S2) and *TaqMan* probes, in Gene Expression Array Cards (Applied Biosystems, Thermo Fisher Scientific, Waltham, MA, EE. UU.) (Table S3) were used. Genes were selected according to LGMDR1 patients' expression profiling [6], however since less zebrafish probes are available, additional muscular genes were included. The CFX384 C1000 thermocycler (Bio-Rad Laboratories, Hercules, CA, EE. UU.) and QuantStudio 12K Flex Real-Time PCR System (Applied Biosystems, Thermo Fisher Scientific, Waltham, MA, EE. UU.) were used. The data were analysed using the Bio-Rad CFX Maestro programme and the ThermoFisher Connect Platform.

RESULTS

The CRISPR/Cas9 technology allows the efficient targeting of the *capn3b* gene.

To achieve a high rate of somatic mutations in F0 zebrafish larvae, we developed a strategy using two sgRNAs targeting distinct coding regions of the *capn3b* gene. Four different sgRNA combinations were designed and tested, with their cutting efficiencies listed in Table S4. Among these, the combination of guides 2 and 3 produced the highest mutation rates across the greatest number of larvae; almost the totality of their genetic material (97.8%) contained mutations in the *capn3b* coding sequence (CDS).

The inactivation of the *capn3b* gene and the treatment with pyrvinium do not affect locomotion.

Our first step in the characterization of *capn3b* crispants was to evaluate how gene inactivation, alongside with the treatment with pyrvinium, influenced larval locomotion.

To achieve this, we tracked the swimming behavior of 144 hpf embryos. By monitoring these behavioral responses under different experimental conditions, we aimed to determine how gene knockout and drug exposure interact to affect larval motility.

We observed that all groups (scrambled and *capn3b* crispants) did not show differences in their response to the environmental illumination changes (Figure 1A).

The inactivation of the *capn3b* gene and the treatment with pyrvinium do not affect muscular integrity.

We characterized the muscular integrity in zebrafish larvae. In healthy zebrafish larvae, the sarcomere structure results in a strong birefringence signal when viewed under polarized light microscopy.

The birefringence of scrambled and *capn3b* crispants was analyzed at three developmental stages: 96, 120 and 144 hpf. We did not detect any differences between the different experimental groups, at any of the concentrations analyzed, suggesting that neither the gene KO nor the drug exposure affected the structure of muscles (Data shown only for 144 hpf, Figure S1).

Gene expression alteration mimic the expression patterns found in LGMDR1.

First of all, we found an interesting finding. We observed that *frzb* expression, highly upregulated in LGMDR1 patients' muscles, was not deregulated in crispant models before administering pyrvinium. Therefore, in our untreated crispant model, as the Wnt signaling pathway inhibitor's expression is not increased, this pathway is not inactivated contrary to what is observed in LGMDR1 patients (Figure 2).

After analysing gene expression, we were able to identify that some of the genes deregulated in the muscle of LGMDR1 patients [5] were also slightly altered in the *capn3b* crispants model. Furthermore, this alteration was increased in the *capn3b* crispants model after treatment with 0.4 µM Pyrvinium, making it more similar to the alterations observed in patients.

There are genes that showed a notably similar profile in the pyrvinium treated *capn3b* crispants model, compared to LGMDR1 patients. Genes that are part of the extracellular matrix, *aspn, col1a1b, col15a1b,* were upregulated in the treated model. In contrast, genes coding for transcription factors (*fos, junbb, jun, jdp2b*) except for *trf1e,* showed significantly reduced expression. Finally, genes encoding for proteins involved in endocytosis (*vldlr*) and cell adhesion (*cd9*) were also upregulated following pyrvinium treatment (Figure 3). Vldlr is a receptor that, by binding to different ligands, participates in lipid metabolism, in a variety of biological functions and acts as a negative regulator of the Wnt signaling pathway [25–28].

The *cd9* gene encodes a cell surface glycoprotein involved in many cellular processes including differentiation, cell–cell fusion events and signal transduction [29, 30]. Additionaly, it has been described in eosinophils' surface [31, 32].

It is worth noting that other genes, deregulated in LGMDR1 patients, showed a similar tendency in their expression, but they did not reach the established threshold of 0.5 fold-change value in the pyrvinium treated knockout model (Figure S2).

DISCUSSION

The generated disease model, with respect to its muscular morphology and function, does not resemble the characteristics observed in LGMDR1 patients. However, it is noteworthy that this model is of great interest due to the rapid generation, made possible by CRISPR/Cas9 technology. This technology has been further demonstrated by other studies to generate zebrafish models for different muscular dystrophies, providing valuable insights into disease mechanisms and potential therapies [33–35].

On the one hand, the lack of *frzb* expression deregulation in the crispant model prior to the treatment, unlike what is observed in LGMDR1 patients' muscles, suggests that Wnt signaling pathway is not inhibited in this model.

This signaling pathway is one of the most relevant for protein synthesis. Given the high protein turnover in the muscle fiber, the impairment of its activity, combined with calpain 3 deficiency, poses an additional limitation for the proper muscle function in LGMDR1 patients. Nevertheless, in our zebrafish model, since the Wnt signaling does not appear to be inhibited, it could be suggested that its maintained activity might enable the model to avoid the dystrophic phenotype. However, further studies are required to confirm this hypothesis.

Based on the alterations in gene expression following pyrvinium treatment, relevant similarities to the LGMDR1 pathophysiology were observed. Fibrosis, the excessive accumulation of connective tissue that replaces the muscle fibers is a hallmark of muscular dystrophies, leading to impaired function and reduces muscular strength. Notably, the increase in collagen expression is not observed in the untreated crispant model. However, the Wnt signaling inhibition induced by drug administration elevates the expression of two types of collagens (*col1a1b*, *col15a1b*), which are also upregulated in LGMDR1 patients [5]. This model could provide a fibrosis-presenting system for future studies.

Regarding the expression of the transcription factors genes, it is important to note that, although their expression is already reduced in the untreated crispant model, this reduction is even more pronounced following drug administration. This finding is particularly relevant, as the strongest downregulation of the transcription factors expression in the patients' muscles is observed along with the most homogeneous downregulation pattern across the biological groups [5].

Finally, among the deregulated genes with distinc functions, it has been reported that the very-low-density lipoprotein receptor (VLDLR) heterodimerizes with LRP6 and that this interaction may represent a novel mechanism for regulating Wnt/β-catenin signaling. Notably, VLDLR negatively regulates Wnt signaling pathway [28, 36, 37]. This observation aligns with the finding in patients and represents an interesting mechanism that require further investigation.

The fact that cd9 is present on the eosinophils surface [31, 32] and that its expression is significantly increased in the treated model is of great interest, especially since eosinophilic infiltration has been identified in LGMDR1 younger patients [38, 39]. This may suggest that, since these zebrafish models are still too young, they could replicate observations seen in younger patients. While it is true that we cannot definitively

demonstrate the presence of eosinophilia, it has been reported a conserved role for eosinophils in the zebrafish [40].

Therefore, the results obtained in the zebrafish model treated with pyrvinium, an inhibitor of the Wnt signalling pathway, support the relevance of Wnt pathway regulation in disease progression.

On the one hand, the absence of clinical or functional characteristics similar to those of LGMDR1 patients makes this model not fully validated for drug evaluation. On the other hand, the improved similarity in gene expression patterns achieved with the drug Pyrvinium paves the way to obtain a potential animal model [18, 41].

However, it is important to note that due to animal experimentation limitations, the study only reached the larval stage at 144 hpf. At this early stage, the fish may not yet exhibit a clear phenotype due to their age [42]. Ideally, to better mimic the clinical onset of the disease in patients [1, 2] a more advanced stage should be reached, such as the juvenile stage (approximately 30 days old) or later. Evaluating these fish at a more mature stage would help to determine if we have generated a truly representative disease model. Therefore, we suggest that subsequent studies are required on juvenile and adult models to confirm the possible phenotype.

Author Contributions: Conceptualization, A.S.; Methodology, C.R.-R., and A.S.; Validation, C.R.-R, J.I., and A.S.; Formal analysis, A.V., C.R.-R., and A.S.; Investigation, A.V., C.R.-R., J.I. and A.S.; Resources, A.S.; Writing—original draft, C.R.-R and A.S.; Writing—review & editing, C.R.-R., A.V., J.I., F.DS, R.F-T, A.L.d.M. and A.S.; Visualization, A.S.; Supervision, A.S.; Project administration, A.S.; Funding acquisition, A.S. All authors have read and agreed to the published version of the manuscript.

Funding: This study was funded by the Instituto de Salud Carlos III (ISCIII) through the project “PI21/00047” and co-funded by the European Union. It was also funded by the Department of Health from the Government of the Basque Country (project ref 2021111022). This work was, in part, supported by the Center for Networked Biomedical Research on Neurodegenerative Diseases (CIBERNED: CB06/05/1126 to Andrea Valls, Jenita Immanuel, Adolfo López de Munain, and Amets Sáenz) and GENE (the Association of Neuromuscular Diseases of Gipuzkoa).

Institutional Review Board Statement: For breeding of zebrafish, ethical approval was obtained from Generalitat de Catalunya “Direcció General de Polítiques Ambientals i Medi Natural” under referential procedure number 18-011-ISA-RESOLUCIO 9421: Breeding of zebrafish (*Danio rerio*) for the maintenance of lines and the creation of transgenics intended to study human diseases.

Acknowledgments: We acknowledge Ana García Durán for her valuable advice and support in the design of the experimental process.

Conflicts of Interest: F.D.S. was employed by ZeClinics SL, a contract research organization providing zebrafish-based services, at the moment of the manuscript preparation.

REFERENCES

[1] Fardeau M, Hillaire D, Mignard C, et al. Juvenile limb-girdle muscular dystrophy Clinical, histopathological and genetic data from a small community living in the Reunion Island. *Brain* 1996; 119: 295–308.

[2] Urtasun M, Sáenz A, Roudaut C, et al. Limb-girdle muscular dystrophy in Guipuzcoa (Basque Country, Spain). *Brain* 1998; 121: 1735–1747.

[3] Sorimachi H, Imajoh-Ohmi S, Emori Y, et al. Molecular cloning of a novel mammalian calcium-dependent protease distinct from both m- and μ-types. Specific expression of the mRNA in skeletal muscle. *Journal of Biological Chemistry* 1989; 264: 20106–11.

[4] Kramerova I, Kudryashova E, Tidball JG, et al. Null mutation of calpain 3 (p94) in mice causes abnormal sarcomere formation in vivo and in vitro. *Hum Mol Genet* 2004; 13: 1373–88.

[5] Sáenz A, Azpitarte M, Armañanzas R, et al. Gene expression profiling in limb-girdle muscular dystrophy 2A. *PLoS One*; 3. Epub ahead of print 2008. DOI: 10.1371/journal.pone.0003750.

[6] Rico A, Guembelzu G, Palomo V, et al. Allosteric modulation of GSK□3β as a new therapeutic approach in limb girdle muscular dystrophy R1 Calpain 3□related. *Int J Mol Sci*; 22. Epub ahead of print 2021. DOI: 10.3390/ijms22147367.

[7] Valls A, Ruiz-Roldán C, Immanuel J, et al. The Role of Integrin β1D Mislocalization in the Pathophysiology of Calpain 3-Related Limb–Girdle Muscular Dystrophy. *Cells* 2025; 14: 446.

[8] Tagawa K. Myopathy phenotype of transgenic mice expressing active site-mutated inactive p94 skeletal muscle-specific calpain, the gene product responsible for limb girdle muscular dystrophy type 2A. *Hum Mol Genet* 2000; 9: 1393–1402.

[9] Richard I, Roudaut C, Marchand S, et al. Loss of Calpain 3 Proteolytic Activity Leads to Muscular Dystrophy and to Apoptosis-Associated Iκbα/Nuclear Factor κb Pathway Perturbation in Mice. *J Cell Biol* 2000; 151: 1583–1590.

[10] Ojima K, Kawabata Y, Nakao H, et al. Dynamic distribution of muscle-specific calpain in mice has a key role in physical-stress adaptation and is impaired in muscular dystrophy. *Journal of Clinical Investigation* 2010; 120: 2672–2683.

[11] Ermolova N, Kudryashova E, DiFranco M, et al. Pathogenity of some limb girdle muscular dystrophy mutations can result from reduced anchorage to myofibrils and altered stability of calpain 3. *Hum Mol Genet* 2011; 20: 3331–3345.

[12] Jaka O, Kramerova I, Azpitarte M, et al. C3KO mouse expression analysis: downregulation of the muscular dystrophy Ky protein and alterations in muscle aging. *Neurogenetics* 2012; 13: 347–357.

[13] Tao T, Shi H, Guan Y, et al. Def defines a conserved nucleolar pathway that leads p53 to proteasome-independent degradation. *Cell Res* 2013; 23: 620–634.

[14] Chen Y, Huang D, Xie A, et al. Capn3b-deficient zebrafish model reveals a key role of autoimmune response in LGMDR1. *Journal of Genetics and Genomics* 2024; 51: 1375–1388.

[15] Guan Y, Huang D, Chen F, et al. Phosphorylation of Def Regulates Nucleolar p53 Turnover and Cell Cycle Progression through Def Recruitment of Calpain3. *PLoS Biol* 2016; 14: e1002555.

[16] Prykhozhij S V., Caceres L, Ban K, et al. Loss of calpain3b in Zebrafish, a Model of Limb-Girdle Muscular Dystrophy, Increases Susceptibility to Muscle Defects Due to Elevated Muscle Activity. *Genes (Basel)* 2023; 14: 492.

[17] Egerman MA, Glass DJ. Signaling pathways controlling skeletal muscle mass. *Crit Rev Biochem Mol Biol* 2014; 49: 59–68.

[18] Bodine SC, Stitt TN, Gonzalez M, et al. Akt/mTOR pathway is a crucial regulator of skeletal muscle hypertrophy and can prevent muscle atrophy in vivo. *Nat Cell Biol* 2001; 3: 1014–9.

[19] Logan CY, Nusse R. The Wnt signaling pathway in development and disease. *Annual Review of Cell and Developmental Biology* 2004; 781–810.

[20] Jaka O, Casas-Fraile L, Azpitarte M, et al. FRZB and melusin, overexpressed in LGMD2A, regulate integrin β1D isoform replacement altering myoblast fusion and the integrin-signalling pathway. *Expert Rev Mol Med*; 19. Epub ahead of print 2017. DOI: 10.1017/erm.2017.3.

[21] Westerfield M. *The zebrafish book. A guide for the laboratory use of zebrafish (Danio rerio)*. 4th ed. University of Oregon: Eugene, OR, USA, 2000.

[22] Rosen JN, Sweeney MF, Mably JD. Microinjection of Zebrafish Embryos to Analyze Gene Function. *Journal of Visualized Experiments*. Epub ahead of print 9 March 2009. DOI: 10.3791/1115.

[23] Locubiche S, Ordóñez V, Abad E, et al. A Zebrafish-Based Platform for High-Throughput Epilepsy Modeling and Drug Screening in F0. *Int J Mol Sci* 2024; 25: 2991.

[24] Berger J, Currie PD. Zebrafish models flex their muscles to shed light on muscular dystrophies. *Dis Model Mech* 2012; 5: 726–32.

[25] Hussain MM, Strickland DK, Bakillah A. THE MAMMALIAN LOW-DENSITY LIPOPROTEIN RECEPTOR FAMILY. *Annu Rev Nutr* 1999; 19: 141–172.

[26] Argraves W, S. Members of the low density lipoprotein receptor family control diverse physiological processes. *Frontiers in Bioscience* 2001; 6: d406.

[27] Tissir F, Goffinet AM. Reelin and brain development. *Nat Rev Neurosci* 2003; 4: 496–505.

[28] Chen Y, Hu Y, Lu K, et al. Very Low Density Lipoprotein Receptor, a Negative Regulator of the wnt Signaling Pathway and Choroidal Neovascularization. *Journal of Biological Chemistry* 2007; 282: 34420–34428.

[29] Tachibana I, Hemler ME. Role of Transmembrane 4 Superfamily (Tm4sf) Proteins Cd9 and Cd81 in Muscle Cell Fusion and Myotube Maintenance. *J Cell Biol* 1999; 146: 893–904.

[30] Le Naour F, Rubinstein E, Jasmin C, et al. Severely Reduced Female Fertility in CD9-Deficient Mice. *Science (1979)* 2000; 287: 319–321.

[31] Akuthota P, Melo RCN, Spencer LA, et al. MHC Class II and CD9 in Human Eosinophils Localize to Detergent-Resistant Membrane Microdomains. *Am J Respir Cell Mol Biol* 2012; 46: 188–195.

[32] Weihrauch T, Melo RCN, Gray N, et al. Eosinophil extracellular vesicles and DNA traps in allergic inflammation. *Frontiers in Allergy*; 5. Epub ahead of print 1 August 2024. DOI: 10.3389/falgy.2024.1448007.

[33] Hu Y, Hruscha A, Pan C, et al. Mis-localization of endogenous TDP-43 leads to ALS-like early-stage metabolic dysfunction and progressive motor deficits. *Mol Neurodegener* 2024; 19: 50.

[34] Donaka R, Zheng H, Ackert-Bicknell CL, et al. Early life lipid overload in Native American Myopathy is phenocopied by stac3 knockout in zebrafish. *Gene* 2025; 936: 149123.

[35] Barraza-Flores P, Moghadaszadeh B, Lee W, et al. Zebrafish and cellular models of SELENON-Congenital myopathy exhibit novel embryonic and metabolic phenotypes. *Skelet Muscle* 2025; 15: 7.

[36] Lee K, Shin Y, Cheng R, et al. Receptor heterodimerization as a novel mechanism for regulation of Wnt/β-catenin signaling. *J Cell Sci*. Epub ahead of print 1 January 2014. DOI: 10.1242/jcs.149302.

[37] Chen Q, Takahashi Y, Oka K, et al. Functional Differences of Very-Low-Density Lipoprotein Receptor Splice Variants in Regulating Wnt Signaling. *Mol Cell Biol* 2016; 36: 2645–2654.

[38] Krahn M, Lopez De Munain A, Streichenberger N, et al. *CAPN3* mutations in patients with idiopathic eosinophilic myositis. *Ann Neurol* 2006; 59: 905–911.

[39] Krahn M, Goicoechea M, Hanisch F, et al. Eosinophilic infiltration related to CAPN3 mutations: a pathophysiological component of primary calpainopathy? *Clin Genet* 2011; 80: 398–402.

[40] Balla KM, Lugo-Villarino G, Spitsbergen JM, et al. Eosinophils in the zebrafish: prospective isolation, characterization, and eosinophilia induction by helminth determinants. *Blood* 2010; 116: 3944–3954.

[41] Thorne CA, Hanson AJ, Schneider J, et al. Small-molecule inhibition of Wnt signaling through activation of casein kinase 1α. *Nat Chem Biol* 2010; 6: 829–836.

[42] Kimmel CB, Ballard WW, Kimmel SR, et al. Stages of embryonic development of the zebrafish. *Developmental Dynamics* 1995; 203: 253–310.

FIGURE LEGENDS

Figure 1. Locomotion Activity Assessment. **(A)** Total distance moved per minute during the dark/light phase. Different experimental conditions are represented in different colors as shown in the legend on the left. Error bars represent the standard error of the mean (SEM). (**B)** Total distance moved during the dark/light transition test. Scrambled is represented in gray, capn3b crispant is represented in red (0.1%DMSO) and the treated with pyrvinium 0.4 μM, in blue. Error bars represent the minimum to maximum values. All comparisons are not significant (One-way ANOVA followed by Sidak's test for multiple comparisons).

Figure 2. Relative expression levels of *frzb* in *capn3b*-/- model and after treatment with pyrvinium. Gene expression was analysed in both untreated control and 0.4 μM Pyrvinium-treated *capn3b*-/- zebrafish samples. Fold change threshold ≥1. Data is normalized to a reference gene, *ef1α*. *TaqMan probe. Error bars represent the minimum to maximum values. Unpaired T-Test was performed to assess statistical significance (*p-value<0.05; ***p-value<0.001 ****p-value<0.0001).

Figure 3. Deregulated genes in *capn3b*-/- model and after treatment with pyrvinium. Data shows the relative expression levels of **A)** Extracellular matrix (*aspn, col1a1b, col15a1b*), **B)** Transcription factors (*fos, junbb, jun, jdp2b, trf1a*), **C)** Cell adhesion genes (*vldlr*) and **D)** Endocytosis genes (*cd9*). Gene expression was analysed in both untreated control and 0.4 μM Pyrvinium-treated *capn3b*-/- zebrafish samples. Fold change threshold ≥1.5 or ≤0.5. Data is normalized to a reference gene, *ef1α*. *TaqMan probes. Error bars represent the minimum to maximum values. Unpaired T-Test was performed to assess statistical significance (*p-value<0.05; **p-value<0.01; ***p-value<0.001 ****p-value<0.0001).

Figure S1. Representative pictures of the birefringence signal of scrambled (left panel) and capn3b crispants (right panel) at 144 hpf. Different concentrations of the pyrvinium treatment are shown in increasing order, from top to bottom (0.1%DMSO; pyrvinium 0.025 μM, pyrvinium 0.05 μM, pyrvinium 0.1 μM, pyrvinium 0.02 μM, pyrvinium 0.4 μM). Scale bar= 100 μm.

Figure S2. Genes with subtle alterations in expression levels in *capn3b*-/- model and after treatment with pyrvinium. Data shows the relative expression levels of *myom3, roraa* and *parvb*. Gene expression was analysed in both untreated control and 0.4 μM Pyrvinium-treated *capn3b*-/- zebrafish samples. Fold change threshold ≥1. Data is normalized to a reference gene, *ef1α*. *TaqMan probes. Error bars represent the minimum to maximum values. Unpaired T-Test was performed to assess statistical significance (*p-value<0.05; ***p-value<0.001 ****p-value<0.0001).

Figure 1

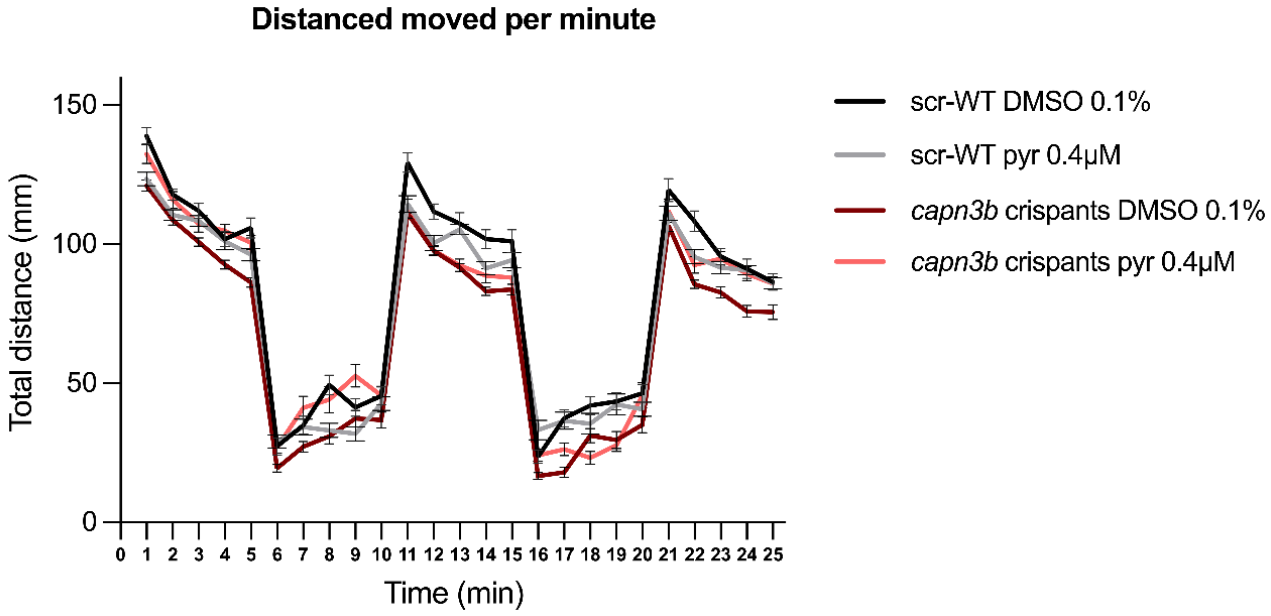
Distanced moved per minute
Total distance (mm)
150
100
50
0
0 1 2 3 4 5 6 7 8 9 10 11 12 13 14 15 16 17 18 19 20 21 22 23 24 25
Time (min)
scr-WT DMSO 0.1%
scr-WT pyr 0.4μM
capn3b crispants DMSO 0.1%
capn3b crispants pyr 0.4μM

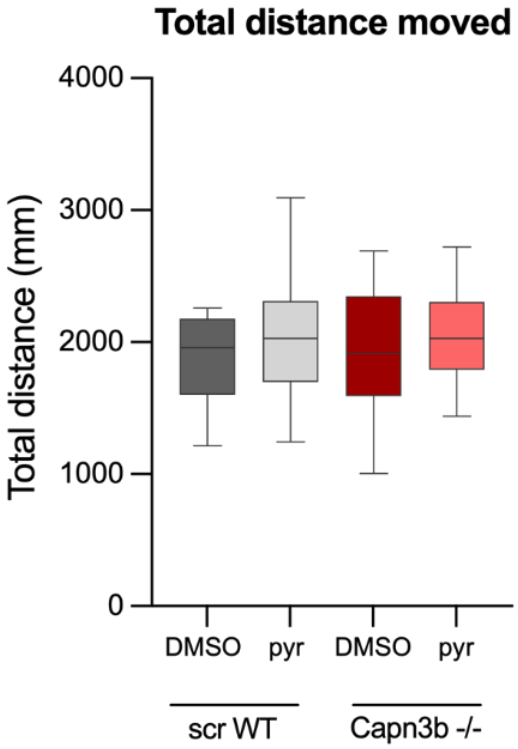
Total distance moved
Total distance (mm)
4000
3000
2000
1000
0
DMSO
pyr
DMSO
pyr
scr WT
Capn3b -/-

Figure 2

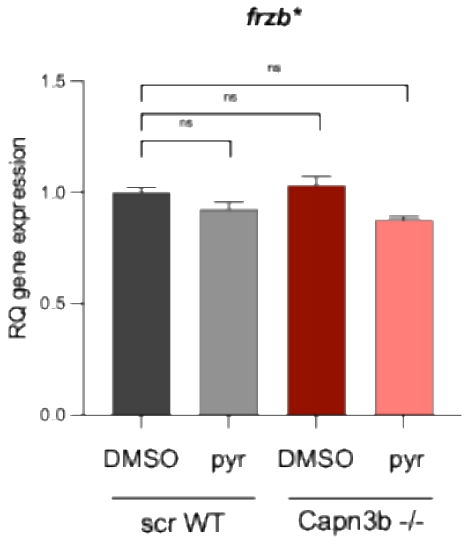
frzb*
ns
ns
ns
1.5
1.0
0.5
0.0
RQ gene expression
DMSO
pyr
DMSO
pyr
scr WT
Capn3b -/-

Figure 3

A) Extracellular matrix

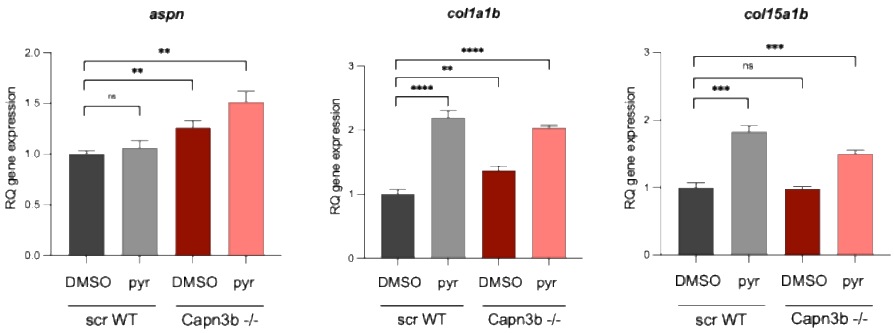

B) Transcription factors

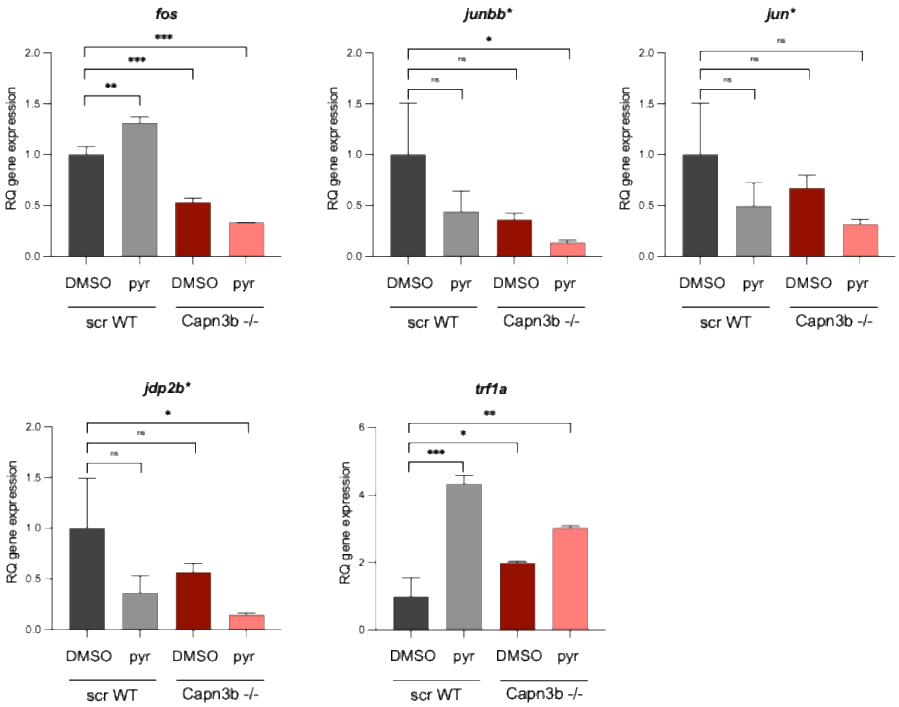

C) Endocytosis genes

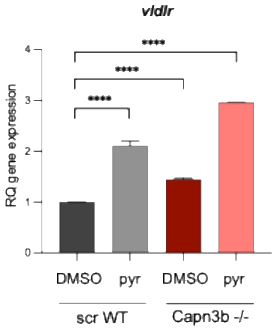

D) Cell adhesion genes

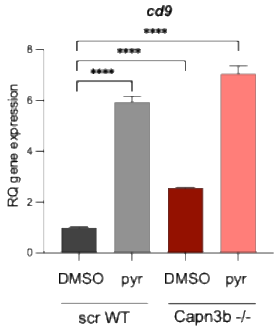

Figure S1

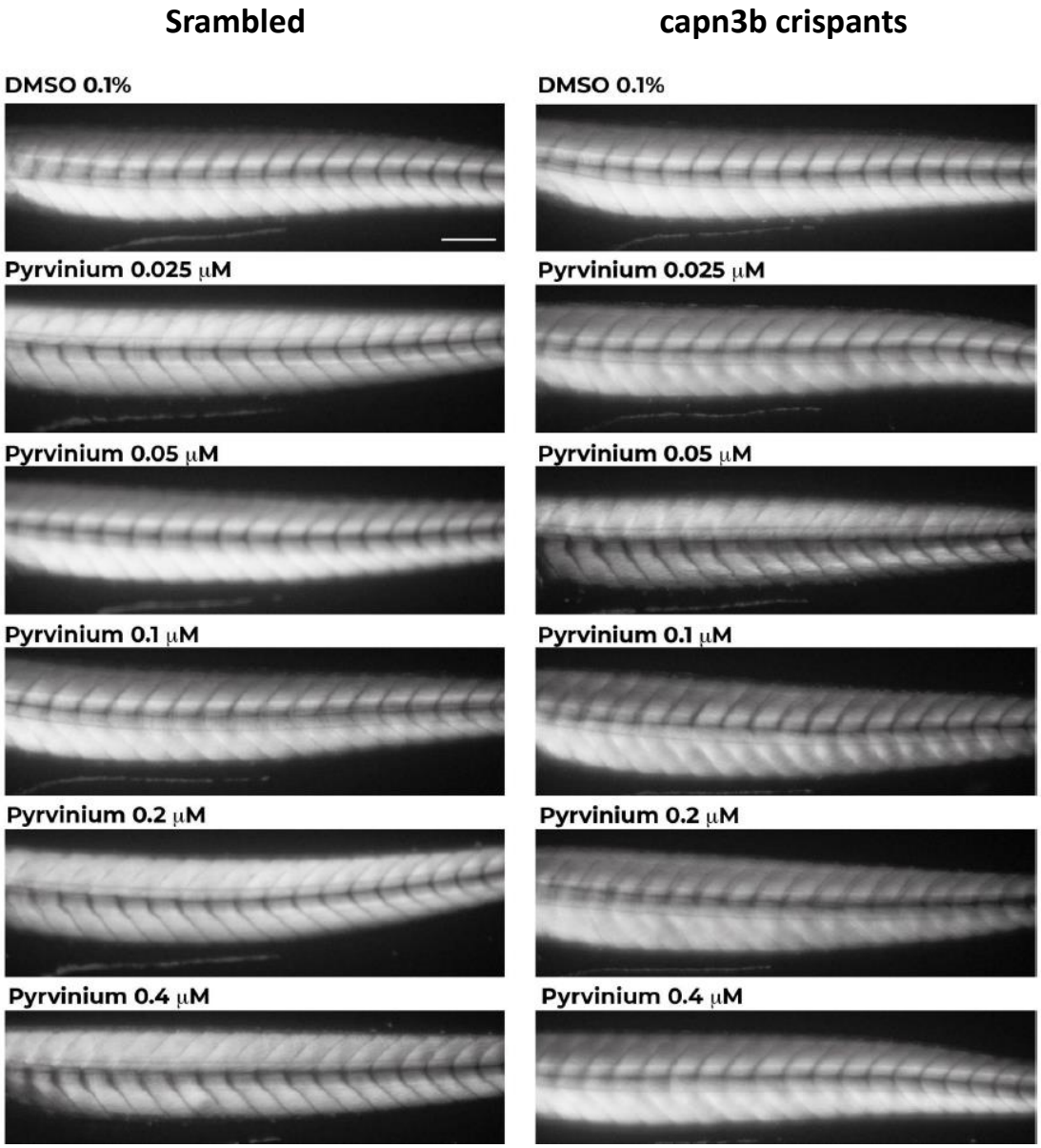

Figure S2

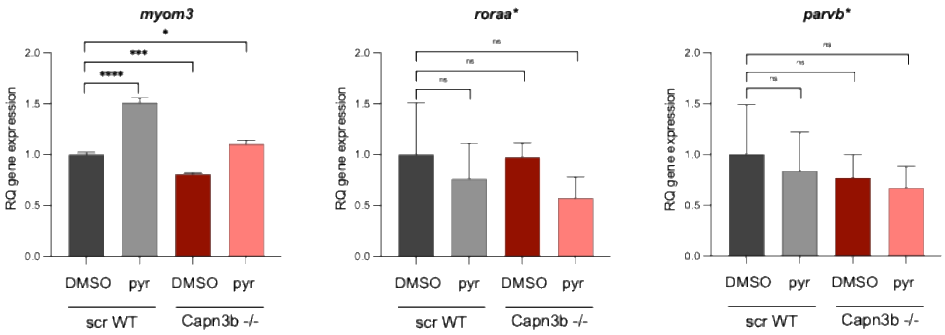

SUPPLEMENTAL MATERIAL

Table S1. Sequences of sgRNA and the corresponding primers for *capn3b* analysis and sequencing.

Zebrafish sgRNAs:	**Sequence**
capn3b-sgRNA1	5'-TCTGTCATCAAAGAGCAATA-3'
capn3b-sgRNA2	5'-GCGGAGCAGCTTCAGTGAGT-3'
capn3b-sgRNA3	5'-AGTTCCCCTTAAAGCTTGAA-3'
capn3b-sgRNA4	5'-CGCTTCCATTCAAGCTTTAA-3'
DNA oligos (PCR primers)	
capn3b-fw	ATTTGTGTACATGAGCAGGGGT
capn3b-rev	CCTCTGACACCTACAGACATTCA

Table S2. Sequences of *SYBR-Green* primers.

Gene symbol	**Gene**	**Sequence**
aspn	***asporin (LRR class 1)***	**F:** ATTCTTCAGGACTAAACCCC **R:** GTAGGGCGAGTAGTAAAAGT
cd9a	***CD9 molecule a***	**F:** TTTCTCCTGAACTCAGTCTT **R:** GAACAAACTCTTGGTCTTGG
col1a1b	***collagen, type I, alpha 1b***	**F:** GATGACATCTCATTCGGTAG **R:** GTTTCCATACATCCTTGTCG
col5a1	*procollagen, type V, alpha 1*	**F:** ACACTGATCAATCTAACCCA **R:** CATGTCCTCATAGTAGGGAT
col15a1b	***collagen, type XV, alpha 1b***	**F:** CATTAACTTCCAGGACCTTT **R:** TTTGTGAGGTTCAGTTTAGC
ctnnb1	*catenin (cadherin-associated protein), beta 1*	**F:** CATTCTAGCCAGAGACATTC **R:** TAGGAGAATACAGCAACTGA
cthrc1a	*collagen triple helix repeat containing 1a*	**F:** AAAGCCAAAGAAAGGATACC **R:** TTTATCCCTGGATTCCCATC
ef1α	*eukaryotic translation elongation factor 1 alpha 1*	**F:** ACCTACCCTCCTCTTGGTCG **R:** AGAACACGCCGCAACCTTTG
fn1b	*Fibronectin 1b*	**F:** GCTACAACCACTTATGAACA **R:** GAGTTAGAGTCCACATCAGT
fos	***v-fos FBJ murine osteosarcoma viral oncogene***	**F:** GACAGGATGATGTTTACCAG **R:** GAACTCCTGAGTCTGGTTG
kal1a	***anosmin 1a***	**F:** CCTCATATCCCAGTCTCAAAT **R:** TAACTGAAGGCCAGAAACTA
myca	*MYC proto-oncogene, bHLH transcription factor a*	**F:** GATTTTACTTCTCGCTCCTTC **R:** ACTTGTGTTTAACGAATGCC
myom3	***myomesin 3***	**F:** CGGCAAGTACCGTATCACCA **R:** ATCTCCGAGTCAAAGCCAGC
tfr1a	***transferrin receptor 1a***	**F:** GCAACTTCAAGGAGTTTTCT **R:** CCCCATGATTTTATTAGCCAG
vldlr	*very low density lipoprotein receptor*	**F:** TGTCACAATGGTTACCAGAT **R:** ATAAGACAGGGCTCTTTACC

Table S3. *TaqMan* probes.

Gene symbol	**Gene Name**	**Assay ID**

18s rRNA	-	Hs99999901_s1
akt2	*v-akt murine thymoma viral oncogene homolog 2*	Dr03119269_m1
aspn	*asporin (LRR class 1)*	Dr03144419_m1
b2m	*beta-2-microglobulin*	Dr03432699_m1
cd9a	*CD9 molecule a*	Dr03133120_m1
cd9b	*CD9 molecule b*	Dr03127057_m1
col15a1a	*collagen, type XV, alpha 1a*	Dr03123974_m1
col1a1b	*collagen, type I, alpha 1b*	Dr03126620_m1
cthrc1a	*collagen triple helix repeat containing 1a*	Dr03089652_m1
ctnnb1	*catenin (cadherin-associated protein), beta 1*	Dr03432620_m1
ctnnb1	*catenin (cadherin-associated protein), beta 1*	Dr03432619_m1
ctnnb1	*catenin (cadherin-associated protein), beta 1*	Dr03432622_m1
desma	*desmin a*	Dr03111913_m1
ef1α	*eukaryotic translation elongation factor 1 alpha 1, like 1*	Dr03432748_m1
fbxo32	*F-box protein 32*	Dr03151496_m1
fhl1a	*four and a half LIM domains 1a*	Dr03422809_m1
fn1b	*fibronectin 1b*	Dr03141145_m1
fosab	*v-fos FBJ murine osteosarcoma viral oncogene homolog Ab*	Dr03100811_g1
fosab	*v-fos FBJ murine osteosarcoma viral oncogene homolog Ab*	Dr03100809_g1
frzb	***frizzled related protein***	Dr03131328_m1
frzb	*frizzled related protein*	Dr03131329_g1
fzd5	*frizzled class receptor 5*	Dr03105573_s1
gpc4	*glypican 4*	Dr03125261_m1
gsk3ab	*glycogen synthase kinase 3 alpha b*	Dr03125061_m1
igf1	***insulin-like growth factor 1***	Dr03105962_m1
ilk	*integrin-linked kinase*	Dr03106934_m1
itgb1a	*integrin, beta 1a*	Dr03091158_m1
itgb1b	*integrin, beta 1b*	Dr03142053_m1
itgb1a	*integrin, beta 1a*	Dr03091156_m1
itgb1b	*integrin, beta 1b*	Dr03142049_m1
jdp2b	***Jun dimerization protein 2b***	Dr03095581_m1
jun	***Jun proto-oncogene, AP-1 transcription factor subunit***	Dr03202188_s1
junba	*JunB proto-oncogene, AP-1 transcription factor subunit a*	Dr03204057_s1
junbb	***JunB proto-oncogene, AP-1 transcription factor subunit b***	Dr03203565_s1
mest	*mesoderm specific transcript*	Dr03144200_m1
mstna	*myostatin a*	Dr03116274_g1
mtor	*mechanistic target of rapamycin kinase*	Dr03085218_m1
mtor	*mechanistic target of rapamycin kinase*	Dr03085224_m1
mtor	*mechanistic target of rapamycin kinase*	Dr03085220_m1
mycb	*MYC proto-oncogene, bHLH transcription factor b*	Dr03132408_g1
myf5	*myogenic factor 5*	Dr03074150_m1
myh7	*myosin heavy chain 7*	Dr03431136_m1

myoc	*myocilin*	Dr03090431_m1
myod1	*myogenic differentiation 1*	Dr03138242_g1
parvb	*parvin, beta*	Dr03093847_m1
parvb	*parvin, beta*	Dr03093843_m1
parvb	***parvin, beta***	Dr03093840_m1
pax7a	*paired box 7a*	Dr03125025_m1
prkaa1	*protein kinase, AMP-activated, alpha 1 catalytic subunit*	Dr03118618_m1
ptk2ab	*protein tyrosine kinase 2ab*	Dr03074223_m1
roraa	***RAR-related orphan receptor A, paralog a***	Dr03442715_m1
slc5a2	*solute carrier family 5 member 2*	Dr03095067_m1
sparc	*secreted protein, acidic, cysteine-rich (osteonectin)*	Dr03146594_m1
tln1	*talin 1*	Dr03128169_m1
tln1	*talin 1*	Dr03128143_m1
tln1	*talin 1*	Dr03128163_m1
tppp3	*tubulin polymerization-promoting protein family member 3*	Dr03075354_m1
vldlr	*very low density lipoprotein receptor*	Dr03437955_m1
wls	*Wnt ligand secretion mediator*	Dr03146331_m1
wnt1	*wingless-type MMTV integration site family, member 1*	Dr03432572_m1
wnt5b	*wingless-type MMTV integration site family, member 5b*	Dr03150114_m1
wnt8b	*wingless-type MMTV integration site family, member 8b*	Dr03131337_m1
wnt9a	*wingless-type MMTV integration site family, member 9A*	Dr03148916_m1

Table S4. sgRNAs cutting efficiency (mean +/- SEM).

	sgRNAs combinations	**Efficiency**
***capn3b* gene**	1+3	94 +/- 4.4
	1+4	49.7 +/- 11.3
	2+3	97.8 +/- 1.9
	2+4	69 +/- 7.9

Table S5. Total distance moved during the trial by each larva.

Experimental group	**Number of larvae**	**Mean (mm)**	**SEM**
Scrambled_DMSO 0.1%	16	1892	81.6
capn3b_DMSO 0.1%	16	1935	113.8
capn3b_pyrvinium 0.4 μM	16	1806	180.6